Published in final edited form as:
Plant Biol (Stuttg). 2011 July ; 13(4): 590–601. doi:10.1111/j.1438-8677.2010.00413.x.

Actin-dependent deposition of putative endosomes and of endoplasmic reticulum during early stages of wound healing in characean internodal cells

A. Klima and **I. Foissner**
Dept. Cell Biology, Div. Plant Physiology, University of Salzburg, Austria

Abstract

We investigated the behaviour of organelles stained by FM1-43 (putative endosomes) and/or LysoTracker Red (LTred; acidic compartments) and that of the endoplasmic reticulum (ER) during healing of puncture and UV-induced wounds in internodal cells of *Nitella flexilis* and *Chara corallina*. Immediately after puncturing, wounds were passively sealed by a plug of solid vacuolar inclusions onto which a bipartite wound wall was actively deposited. The outer, callose-containing amorphous layer consisted of remnants of FM1-43- and LTred-labelled organelles, of ER cisternae and of polysaccharide-containing secretory vesicles which became deposited in the absence of membrane retrieval (compound exocytosis). During formation of the inner, cellulosic layer exocytosis of secretory vesicles with the newly formed plasma membrane is coupled to endocytosis via coated vesicles. Migration of FM1-43- and LTred-stained organelles, of ER and of secretory vesicles towards the cell cortex and the deposition of a bipartite wound wall could also be induced by spot-like irradiation with ultraviolet light. Cytochalasin D reversibly inhibited the accumulation and deposition of organelles. Our study indicates that active, actin-dependent deposition of putative recycling endosomes is required for wound healing (plasma membrane repair) and supports the hypothesis that deposition of ER cisternae helps to restore wounding-disturbed Ca^{2+} metabolism.

Keywords

Chara; cytoskeleton; endocytosis; exocytosis; *Nitella*; plant; plasma membrane repair; wound wall

INTRODUCTION

The Characeae are multicellular green algae and morphological, biochemical, and molecular data strongly suggest that they are close to the common ancestor of green algae and higher plants (Graham *et al*. 2000; Turmel *et al*. 2007). The upward growing thallus consists of a regular alternation of groups of small nodal cells and huge internodes which may grow up to 20 cm in length by diffuse elongation. The internodal cells are well known for their rapid cytoplasmic streaming which depends on interaction of myosin-coated organelles with parallel, subcortical actin bundles attached to the inner surface of stationary chloroplast files (Figs. 1A and B; Shimmen & Yokota 2004). They have been and still are a valuable experimental tool for investigating the plant cytoskeleton and for the study of local wound responses (Foissner & Wasteneys 2000). The cells readily react to damage caused by mechanical wounding, chemical treatment or UV irradiation and, depending on the type and

Correspondence I. Foissner, Dept. Cell Biology, Div. Plant Physiology, University of Salzburg, Hellbrunnerstrasse 34, A-5020 Salzburg, Austria. ilse.foissner@sbg.ac.at.

Europe PMC Funders Author Manuscripts

severity of wounding, different types of wound walls are secreted. Membrane- and callose-containing “amorphous” wound walls have been described from cells injured by Ca^{2+} ionophores and membrane-free, cellulosic wound walls were found after puncturing or after treatment of cells with high concentrations of $CaCl_2$ (Foissner 1988a; b; 1990). Wound healing requires transient reorganization of the parallel subcortical actin bundles into a meshwork of randomly oriented filaments which guarantees transport and exocytosis of wall forming secretory vesicles (Foissner *et al*. 1996). The wounding-induced transient polarization of the cell resembles the situation in tip-growing cells where exocytosis and endocytosis are targeted to the apex as long as these cells elongate (Samaj *et al*. 2006).

The actin cytoskeleton has also been implicated in endocytosis i.e. in the process of membrane internalization of animal, fungal and plant cells (Baluska *et al*. 2002; Engqvist-Goldstein & Drubin 2003; Ayscough 2005; Ovecka *et al*. 2005; Voigt *et al*. 2005; Sun *et al*. 2006; Galletta and Cooper 2009). Many of these studies used FM-dyes which insert into the plasma membrane and gradually appear in compartments where they colocalize with various endosomal markers (for recent reviews see Geldner and Jürgens 2006; Robinson *et al*. 2008; Ebine *et al*. 2009). In internodal cells of the characean alga *Chara corallina* internalization of FM1-43 and FM4-64 is active but cannot be inhibited by drugs which affect the actin cytoskeleton (Klima & Foissner 2008). Whether this is due to actin-independent endocytosis or to endocytosis-independent internalization remains as yet unknown. Some of the FM-labelled organelles are also stained by neutral red and lysotracker dyes, indicative of endosomal, acidic compartments (Klima & Foissner 2008) and colocalize with antibodies against endosomal proteins (own unpublished results). Therefore, irrespective of the uptake mechanism, the FM dyes are at least suited for monitoring the distribution and dynamics of endocytic organelles in characean internodal cells. In higher plant cells FM-dyes appear to be taken up via vesicular endocytosis (Dhonukshe *et al*. 2007; Griffing 2008; Van Gisbergen *et al*. 2008) but artefacts due to FM-staining have also been reported (Jelinkova *et al*. 2010).

In the present study we investigated the behaviour of various organelles during healing of puncture and UV-induced wounds. We found that the wound walls consist of two layers, an outer membrane containing, amorphous layer which forms by active, actin-dependent deposition of organelles in the absence of membrane recycling, and an inner, membrane-free homogeneous layer which is similar to the normal cell wall. Our data indicate that putative recycling endosomes are required for plasma membrane repair and add support to the hypothesis that the deposition of ER cisternae is an efficient mechanism to restore wounding-disturbed Ca^{2+}-homoeostasis.

MATERIAL AND METHODS

Plant material, culture conditions and wounding

Shoots of *Nitella flexilis* L. (Ag.) and *Chara corallina* Klein ex Willd., em. R.D.W. were grown in a substrate of soil, peat and sand in 10-50 litre aquaria filled with distilled water. The temperature was about 20 ° C and fluorescent lamps provided a 16/8h light/dark cycle. Non-elongating, mature internodal cells of the main axis or the branchlets were harvested 1 d prior to experiments, trimmed of neighbouring internodal cells and left overnight in artificial fresh water (10^{-3} M NaCl, 10^{-4} M KCl, 10^{-4} M $CaCl_2$).

Cells were wounded with tungsten needles sharpened by repeated immersion into boiling potassium nitrate, or by repeated scanning with the 375 nm laser light of the CLSM (see below).

In vivo staining and inhibitor treatments

Cells were pulse labelled for 10 min with 10 μM FM1-43 (N-(3-triethylammoniumpropyl)-4-(4-(dibutylamino)styryl)pyridinium dibromide; Invitrogen), an endocytic marker, diluted from a 500 μM stock solution in distilled water. The acidotropic dye LysotrackerTred DND-99 (LTred; Invitrogen; 1 mM stock solution in dimethyl sulfoxide (DMSO) was used at 1 μM. The staining patterns obtained with LTred in characean internodal cells varied between lots. Some of them labelled not only small, roundish organelles and vacuoles but also parts of the inner ER. For this study we used lot no. 29709W which did not appear in ER cisternae. Mitochondria were stained with a 1 μM solution of Mitotracker orange CMTMRos (Invitrogen; 1 mM stock solution in DMSO). The ER was visualized by 1 μM freshly prepared 3, 3′ dihexyloxacarbocyanine iodide ($DiOC_6$; Invitrogen; 10 mM stock solution in DMSO). LTred, Mitotracker orange and $DiOC_6$ were applied for 30 min. LTred- and $DiOC_6$-stained cells were washed for 10 min in artificial fresh water before use, Mitotracker orange-labelled cells were washed up to 30 min in order to reduce unspecific cell wall staining.

Calcofluor white (Sigma; 0.1 %) and purified aniline blue (Biosupplies, Melbourne; 0.03 mg/ml) were used to identify cellulose and callose, respectively.

Cells were exposed to 5 μM (*C. corallina*) or 30 μM (*N. flexilis*) cytochalasin D (CD; Sigma; stock solution 10 mM in DMSO), 50 μM latrunculin B (Calbiochem, San Diego, CA, USA; stock solution 10 mM in DMSO) and 50 mM 2,3-butanedione monoxime (BDM; Sigma). Inhibitors were applied 30 min before, during and after wounding.

All dyes and inhibitors were diluted with artificial fresh water. Controls contained up to 1 % DMSO or 2 % ethanol which had no visible effect on cytoplasmic streaming, wound healing or internalization of FM1-43.

Confocal scanning microscopy

The confocal laser scanning microscopes (CLSMs) used in this study were a Zeiss (Jena, Germany) LSM 510 coupled to an Axiovert inverted microscope and a Leica (Mannheim, Germany) TCS SP5 coupled to a DMI 6000B inverted microscope.

FM1-43 and $DiOC_6$ were excited with the 488 nm argon laser line and the resulting emission wavelengths were collected between 505 and 530 nm. LTred and Mitotracker orange were excited with the 561 nm DPSS-laser line and emission wavelengths were collected between 592-656 nm. Calcofluor white and aniline blue were excited with a 375 nm DPSS-laser line and emissions were recorded between 400 and 510 nm. These dyes were either applied on intact cells or on cell wall fragments.

Colocalizations were studied with sequential scan settings to avoid cross-talk between channels. Appropriate controls were made for all single, double and triple labelling experiments in order to exclude bleed through and to distinguish signals from background fluorescence. Observations times were usually restricted to two hours in order to avoid toxic effects or redistribution of fluorescent dyes. Cells were first stained with $DiOC_6$, LTred or Mitrotracker orange for 30 min and after a brief wash in AFW pulse-labelled with FM1-43 for 10 min. After a 20 min wash in AFW these cells were punctured and analysed in the CLSM. We also investigated internodal cells which were pulse labelled with FM1-43 for 10 min and subsequently stained with LTred for 30 min. The results were similar for both staining protocols.

Organelle dynamics and deposition were studied by analysing time series taken at minimum laser intensity and pixel time in order to avoid photobleaching and stress response. The velocity of organelles was calculated from time series taken at 8.8 s intervals.

UV-induced wounds were produced by repeated scanning with the 375 nm line of a laser diode at maximum intensity and at a pixel time of 0.05 ms. The laser light was focused onto the outer surface of the stationary chloroplasts near the plasma membrane and the irradiated area measured between 100 and 700 μm^2. Irradiation for 4-6 min was sufficient to induce wound wall deposition. For quantitative measurements (see below) visible laser lines were switched off during UV-treatment in order to avoid photobleaching of FM1-43, $DiOC_6$ and LTred.

Images produced by the LSM software were further processed with Adobe Photoshop (Adobe Systems) or Amira (Visage Imaging, Berlin, Germany). All images presented in this study are single sections unless otherwise stated. Images of cells are positioned with vertical sides parallel to the long axes of the internodes.

Quantification of wounding-induced deposition of fluorescent material

Internodal cells were stained as indicated above and briefly washed in AFW. Z-stacks with suboptimal settings for photomultiplier gain were taken immediately after puncturing or UV-irradiation and at indicated time intervals with identical instrument settings. Optical sections were produced with minimum laser intensity and pixel time in order to avoid photobleaching.

Volume fractions occupied by fluorescent organelles were calculated from Z-series using Amira software (Visage Imaging, La Jolla, USA). Differences between means of at least 3 cells were analysed by t-test and considered to be significant if $P<0.01$ (Sachs 1984).

Electron Microscopy

Thalli were chemically fixed with 2 % glutaraldehyde dissolved in 0.1 M phosphate buffer, pH 7, postfixed in 1 % OsO_4 (both from Sigma) and further processed as described (Foissner 1988b). Sections were examined in a Zeiss (Oberkochen, Germany) Leo electron microscope.

Polysaccharides were localized according to Thiery's method (Plattner & Zingsheim 1987). Sections of chemically fixed cells were mounted on formvar coated gold grids, oxidised in 1 % periodic acid, washed in distilled water, incubated in 0.2 % thiocarbohydrazide in 20 % acetic acid for 2-12 hours, washed in dilute acetic acid and distilled water, incubated in 1 % aqueous silver proteinate for 30 min, washed in distilled water and viewed without further staining. Silver proteinate was omitted on control sections.

RESULTS

Untreated internodal cells and wound healing in characean algae

For our study we used internodal cells of *Nitella flexilis* which were the subject of several light and electron microscopic studies about wound healing (Foissner 1988a; b; 1990) and internodal cells of *Chara corallina* in which we investigated internalization of FM-dyes (Klima and Foissner 2008).

In internodal cells of *C. corallina* FM1-43 accumulated in numerous distinct patches at or near the plasma membrane within 5 minutes after dye addition (Klima & Foissner 2008). The plasma membrane of *N. flexilis* internodal cells was more homogenously labelled and only few FM1-43-stained structures were seen in the periphery of the cell (Fig. 1A). Five

min after dye addition, fluorescent particles appeared between the stationary chloroplasts (Fig. 1 A and B) and later in the streaming endoplasm. In *N. flexilis* FM-internalization was sensitive to KCN but independent of the actin cytoskeleton as described for *C. corallina* (not shown; Klima & Foissner 2008). LTred, an acidotropic dye, labelled the solid vacuolar inclusions which formed the wound plug and small organelles with a diameter of up to 1 μm (Fig. 1C-E), the membranes of cytoplasmic vacuoles and the membrane of the large central vacuole (not shown). In double labelled cells, between 10 and 50 % of the fluorescent organelles were stained by both dyes (compare Klima & Foissner 2008 and Fig. 1E).

Wound repair after puncturing or UV-irradiation was similar in both species and the resulting wound walls were indistinguishable (Foissner 1988b; Homblé & Foissner 1993). The time required for wound healing, defined by the regeneration of continuous actin bundles and the recovery of active cytoplasmic mass streaming, depended on the size of the wound. Small wounds usually healed within one hour, healing of larger wounds required up to several hours. In the following, the process of wound healing is illustrated for *N. flexilis*. We show that irrespective of the type of damage FM1-43- and LTred-stained organelles and cisternae of the ER are deposited as an outer wound wall before a cellulosic inner wound wall is secreted.

Deposition of putative endosomes and acidic compartments at wounds

Puncturing locally destroyed the cell wall, the plasma membrane and the cortical cytoplasm including the chloroplast files and the subcortical actin bundles. The wound plug contained solid vacuolar inclusions intermingled with fluorescent material which probably derived from FM1-43- and/or LTred-stained organelles passively pushed out of the cell (Fig. 1C and E). During the following minutes numerous FM1-43- and/or LTred-labelled organelles which had a diameter of up to 1 μm accumulated in the non-streaming, stagnant wound cytoplasm (Fig. 1E and F). These organelles did not form at the wound surface but arrived passively at the wound due to local interruption of cytoplasmic streaming and continuous supply of endoplasm from undisturbed upstream regions. After about 10 min they started to perform saltatory movements in various directions towards and away from the wound surface (Suppl. Movie 1). Short periods of continuous movement with a maximal velocity of 15 $\mu m.s^{-1}$ alternated with periods of trembling or oscillating movements. The behaviour of these organelles was similar to that of the polysaccharide-containing secretory vesicles which can be visualized by bright field or DIC (Foissner *et al.* 1996; Fig. 1G, compare with the electron microscopical Fig. 5A and B). These vesicles do not carry FM-fluorescence in unwounded control cells as long as the observation time is restricted to 2 hours (Klima & Foissner 2008). At puncture wounds, however, up to 30 % of the secretory vesicles were labelled by FM1-43 (Fig. 1F and G) and this percentage might even be higher in view of the different thicknesses of optical sections. Many of the FM1-43- and/or LTred-stained organelles and the secretory vesicles became immobilized, clumped together and formed a strongly fluorescent layer which covered the inner surface of the wound plug and neighboured, probably damaged chloroplasts (Figs. 1C-J). This outer wound wall was mostly stained by both dyes, but there were also regions which fluoresced only green or red (Fig. 1C).

We next investigated UV-induced wounds where the cell wall remains intact and which thus offer superior imaging conditions. Using a 375 nm UV laser and a high numerical aperture lens (63x, nA 1.4) we observed a nearly immediate, spectacular invasion of numerous FM1-43- and/or LTred-stained organelles and of secretory vesicles into the cortex of the irradiated area (Fig. 1K-O; Suppl. Movies 2 and 3). The organelles migrated from the slowly, probably passively streaming endoplasm, through the chloroplast layer towards the cell periphery where they performed saltatory movements. After about 4 min, many of the fluorescent organelles and the secretory vesicles became immobilized and deposited in the

cortical cytoplasm of the irradiated area, between the plasma membrane and the outer surface of the detaching chloroplasts (Fig. 1L-O). As observed at puncture wounds, up to 30 % of the FM1-43-labelled organelles colocalized with putative secretory vesicles visible with DIC (not shown). The LTred-fluorescence in the outer wound wall was often weaker than that of the FM1-43-fluorescence suggesting that most of the LTred-stained organelles returned into the cytoplasm (but see discussion). The deposition of organelles in the cell cortex ceased immediately after the UV Laser was switched off but saltatory movements continued for up to one hour in the wound area (see below).

ER cisternae involved in early stages of wound healing

Earlier studies suggested that the ER plays an important role during wound healing in characean internodal and other cells (Foissner 1998 and references therein). In unwounded internodes the ER consists of a mesh-like cortical ER sandwiched between the plasma membrane and the stationary chloroplast files and tubular, branched cisternae which move rapidly along the subcortical actin filament bundles (Fig. 2A-C). The cortical ER in the non-elongating, mature internodal cells used for puncturing consisted of wide meshes which had a random orientation and which changed shape and size only rarely (Fig. 2A; compare Foissner *et al.* 2009). Puncturing locally destroyed the cortical ER and arrested active translocation of ER tubes. The remnants of the cortical and subcortical ER damaged during puncturing remained visible between the solid inclusions of the wound plug and between chloroplasts but during the following minutes additional $DiOC_6$-stained membranes were deposited at the wound plug and around cortical, probably damaged chloroplasts (Fig. 2D-F) until a nearly continuous sheet covered the inner wound surface as illustrated in a 3D-model (Fig. 3H). The fluorescent material was delivered by cisternae of the inner ER which accumulated at the wound due to supply from unwounded control regions (compare Suppl. Movie 5). Cells in which this inner ER was clearly visible showed a reticulate meshwork (Fig. 2E) which moved slowly towards the downstream end of the wound where it became tubular when it contacted the subcortical actin bundles in undisturbed regions.

At UV-induced wounds ER cisternae started to move from the slowly streaming endoplasm towards the plasma membrane after about three minutes irradiation when chloroplasts detached from the cortex. As described above, cisternae were deposited near the remnants of the cortical ER and became a component of the outer wound wall (Fig. 2G-I; Suppl. Movie 5).

Secretion of the inner wound wall

After the deposition of the outer wound wall the abundance of mobile, FM1-43-fluorescent or LTred-stained organelles in the punctured or the UV-irradiated area decreased gradually although secretory vesicles were still present in large numbers and performed salutatory movements (Fig. 3A and B). They often appeared to be embedded in a “cloud” of diffuse FM1-43-fluorescence, which may indicate the presence of minute organelles with a size beyond the diffraction limit of the microscope (not shown). During that stage a non-fluorescent inner wound wall was secreted. At puncture wounds the inner wound wall became up to 5 μm thick (Fig. 3C-G) conferring the necessary stability required for healing cell wall lesions. The newly formed plasma membrane beneath the inner wound wall carried the FM1-43-fluorescence although cells were pulse labelled **before** wounding (Fig. 3E). The inner wound wall at UV-induced wounds had a maximum thickness of 500 nm (compare Foissner 1988a; 1990). Therefore, the FM1-43-fluorescence of the plasma membrane overlapped with that of the outer wound wall and could only be recognized after plasmolysis (not shown). Plasma membrane labelling by LTred or $DiOC_6$ was never observed. After wall deposition was completed, most of the FM1-43- and LTred-stained organelles as well as secretory vesicles disappeared from the wound area and participated in unidirectional

cytoplasmic streaming along the regenerated subcortical actin bundles (compare Foissner *et al.* 1996). The ER beneath healed wounds consisted of a cortical, rather immobile meshwork and of fast moving inner tubes (not shown).

Polysaccharide composition of wound walls

In order to get more information about the chemical composition of the wound walls we used aniline blue, specific for beta 1,3 glucans (Stone *et al.* 1984) and calcofluor, which preferentially binds to cellulose fibres (Herth & Schnepf 1980). Unfortunately, both dyes have similar excitation and emission spectra and can thus not be used for simultaneous labelling of these polysaccharides to reveal their distribution. Therefore, healed wounds were first stained with aniline blue and, after recording the staining pattern (and bleaching of aniline blue-fluorescence) labelled with calcofluor. The aniline blue-fluorescent callose always appeared in the outer wound wall where it partly colocalized with the FM1-43-deposits (Fig. 3C-G, I-L) and the LTred- and $DiOC_6$-fluorescent material (not shown). Calcofluor-labelled cellulose was restricted to the inner wound wall (Fig. 3 C, D, H-J) which was continuous with the cell wall of unwounded control regions (Fig. 3H).

Deposition of putative endosomes and ER at wounds is inhibited by CD

We described previously that the deposition of the fibrillar, cellulosic wound wall (here referred to as inner wound wall) at puncture wounds can be prevented by CD and by BDM which interfere with the actin cytoskeleton and its motor proteins, respectively (Foissner & Wasteneys 1997). During the course of this study we found that the earlier stage of wound healing, i. e. the deposition of an outer, amorphous wound wall is also actin-dependent.

As described above the dynamics and trajectories of FM1-43-labelled organelles in the wound area were similar to those of the secretory vesicles suggesting that they moved along the wounding-induced, CD-sensitive actin meshwork (Foissner *et al.* 1996). CD added to labelled cells before and after puncturing indeed inhibited their accumulation and their dynamics. FM1-43-fluorescent material was present at wounds immediately after puncturing but its volume did not increase during the following hours (Fig. 4A). When these CD-treated cells were transferred into inhibitor-free artificial fresh water, cytoplasmic streaming in unwounded regions recovered within minutes. Numerous FM-stained organelles and unstained secretory vesicles then accumulated at the wound and performed saltatory movements while the intensity and volume of the fluorescent outer wound wall increased significantly (Fig. 4B and C; Table 1). Finally a non- or weakly fluorescent inner wound wall was deposited (not shown). In comparison, the intensity and volume of FM1-43-fluorescent material at wounds decreased (bleached) when internodal cells were not allowed to recover and remained in the CD-containing medium for the same time period (Table 1).

CD also inhibited the accumulation and deposition of LTred-stained particles and of ER cisternae at puncture wounds (not shown but see below) and the migration and deposition of FM1-43-labelled organelles (Fig. 4D), of secretory vesicles (Fig. 4E), of ER cisternae (Fig. 4F) and of LTred-stained particles (not shown) at UV-induced wounds.

The deposition of a bipartite wound wall was also prevented by treatment with 50 mM BDM which reduced cytoplasmic streaming to 20.4±13.3 % (mean±SD; n = 6) of the control rate in branchlet internodal cells of *N. flexilis* within 30 minutes. The BDM-effect, however, was not reversible and cells died within few hours after puncturing (data not shown). Latrunculin B at 50 nM for two hours has little effect on the integrity of the subcortical actin filament bundles and the velocity of cytoplasmic streaming but disrupts the cortical actin filaments near the plasma membrane (Foissner & Wasteneys 2007). This treatment did not interfere with the dynamics of organelles at wounds and the deposition of a wound wall suggesting

that the wound-induced actin meshwork is more stable than the cortical actin filaments in control regions and that latrunculins do not or only weakly affect actin polymerization in characean algae (not shown).

Mitochondria are not directly involved in wound repair

The inhibitor experiments proved that transport and deposition of putative endosomes, ER cisternae, acidic and secretory vesicles at wounds were actin-dependent. We next investigated whether these compartments were specifically involved in early stages of wound healing or whether there was a general delivery and deposition of organelles at wounds. In internodal cells which were labelled with Mitotracker orange prior to puncturing or UV-treatment mitochondria were present between the cortical chloroplasts of unwounded regions and in the streaming endoplasm. A previous study has shown that cortical mitochondria in mature intermodal cells move along actin filaments (Foissner 2004). In spite of that, mitochondria were rarely observed in the cytoplasm near puncture wounds and did not migrate towards UV-irradiated areas (Suppl Movie 4) in striking contrast to the secretory vesicles or the FM1-43-labelled organelles (Suppl. Movie 2). Mitochondria were also completely absent from puncture and UV-induced wound walls (Fig. 4G-I).

LTred-labelled vacuoles and nuclei were also excluded from the cytoplasm adjacent to healing wounds (compare Fig. 1E) and electron micrographs show that peroxisomes, Golgi bodies and multivesicular bodies are not directly involved in wound healing (see below). These data suggest that there is no “mass” deposition of cytoplasm at wounds.

Fine structure of wound walls

The outer wound wall adjacent to the wound plug and damaged chloroplasts in punctured cell or adjacent to the intact cell wall at UV-irradiated areas consisted of amorphous material and abundant membrane residues (Fig. 5A-D). It contained polysaccharides as revealed by silver deposits produced by Thiery’s method (Fig. 5B; Plattner & Zingsheim 1987). They were delivered by the Golgi-derived secretory vesicles which have a characteristic dense core after conventional chemical fixation (Fig. 5A; Franceschi & Lucas 1981). The larger ones corresponded to those organelles which can be visualized by DIC (Fig. 1G; Foissner *et al.* 1996). According to the observations in the CLSM the wound cytoplasm is also populated with numerous FM1-43- and LTred-stained fluorescent organelles which are deposited onto the inner surface of the wound plug. Possible candidates are vesicles with a diameter between 100 and 500 nm which have a homogeneous electron-dense or electron-lucent content after chemical fixation (Fig. 5A, arrows). The latter are, however, difficult to discriminate from cross-sectioned ER cisternae. Putative fusion stages between secretory and other vesicles were occasionally observed in the wound cytoplasm (Fig. 5B). Irrespective of the identity of the organelles involved in wound repair, the presence of membranes within the outer wound wall indicated that deposition of organelles in early stages of wound healing was not linked with membrane recycling. Mitochondria, Golgi bodies, peroxisomes, multivesicular bodies or nuclei were neither observed in the wound cytoplasm nor in the outer wound wall.

Thirty to sixty minutes after puncturing or few minutes after the end of UV-irradiation, a continuous plasma membrane with numerous coated pits (up to 40 per μm^2) and coated vesicles was present while the inner wound wall was secreted (Fig. 5B). Silver deposits at coated pits and coated vesicles indicated that these organelles may not only be involved in plasma membrane internalization but also in polysaccharide recycling (Fig. 5B; compare Dhonukshe *et al.* 2006). The inner wound wall was devoid of membrane residues and its fine structure (Fig. 5C) as well as the chemical composition (see above) was similar to that of the normal cell wall. The plasma membrane beneath healed wounds was smooth; coated pits

and coated vesicles were only occasionally seen (Fig. 5 C; for further details see Foissner 1988b; 1992).

DISCUSSION

A bipartite wound wall is deposited onto puncture and UV-induced wounds

Effective wound healing is essential for cell survival, especially for sessile organisms. In plant cells, rapid deposition of a wound wall is required for the repair of mechanical damage and plays an important role in the defence against pathogens (e. g. Takemoto *et al.* 2006). In spite of its importance, little is known about wound healing in higher plants or green algae as compared with the wealth of data available from the animal kingdom (Schapire *et al.* 2009).

In the present study we investigated the behaviour of various organelles during healing of puncture or UV-induced wounds in internodal cells of the characean green algae. We observed that irrespective of the type of damage wound healing is a biphasic process which involves (1) deposition of an outer wound wall during which putative endosomes, acidic compartments, secretory vesicles and ER cisternae fuse with each other in the absence of membrane recycling and (2) the secretion of an inner wound wall during which exocytosis of secretory and other vesicles is coupled to endocytosis via coated vesicles (Fig. 6). Our data indicate that wound healing does not simply involve site-directed accumulation ("mass flow") of cytoplasm but specific, actin-dependent transport of organelles involved in wound repair. Among those, putative recycling endosomes appear to be essential for plasma membrane repair, a prerequisite for the exocytosis-dependent deposition of the cellulosic inner wound wall. The deposition of ER cisternae may help to restore normal Ca^{2+} levels.

Putative endosomes involved in plasma membrane repair

An outstanding question for wound healing in plant cells is the identification of the nature of cytoplasmic compartments involved in plasma membrane repair (Schapire *et al.* 2009). Immediately after mechanical injury or UV-irradiation, FM1-43- and LTred-stained organelles as well as $DiOC_6$-labelled ER cisternae and secretory vesicles moved towards the damaged area and were actively deposited. The bright FM1-43, LTred and $DiOC_6$-fluorescence of this outer wound wall suggests that the labelled membranes are not recycled consistent with electron micrographs showing abundant membrane residues between clumps of polysaccharides delivered by secretory vesicles. A similar "compound exocytosis" (Pickett & Edwardson 2006) occurs at pathogen-induced papillae of higher plant cells where FM4-64-stained membrane material colocalizes with callose and defence-related proteins (Meyer *et al.* 2009). The fact that the regenerated plasma membrane at wounds carries the FM1-43 fluorescence although cells were pulse-labelled **before** injury indicates that the newly formed plasma membrane is – at least partly – delivered by FM1-43-stained endosomal compartments. The fact that mitochondria, peroxisomes, Golgi bodies, multivesicular bodies and nuclei were neither seen in the cytoplasm near healing wounds nor within the outer wound layer indicates that deposition of organelles during wound healing is specific and involves only compartments which are directly required for wound repair.

The absence of late endosomes (multivesicular bodies and vacuoles) from the wound cytoplasm suggests that the FM1-43-stained organelles involved in plasma membrane repair correspond to the ill defined "recycling endosomes". Recycling endosomes are considered to develop, at least partly, from the trans-Golgi network (Geldner & Jürgens 2006) which is also involved in the formation of secretory vesicles in characean internodal cells (Franceschi & Lucas 1981). The recycling endosomes are probably responsible for the rapid staining of

Europe PMC Funders Author Manuscripts

nascent cell plates by FM4-64 (Dettmer *et al.* 2006; Reichardt *et al.* 2007). Our study indicates that these compartments are also involved in plasma membrane repair at wounds.

The FM1-43-stained organelles implicated in plasma membrane repair may differ in the degree of acidification as indicated by the variable amount of colocalization with LTred (Dettmer *et al.* 2006). We observed also particles which were stained by LTred only and which were also secreted into the outer wound wall, especially after puncturing. The absence of the endocytic marker FM1-43 suggests that these organelles are not part of the endocytic pathway and further work is needed to clarify their identity. However, the results obtained with LTred must be cautiously interpreted. LTred bleaches fast, its specifity is under discussion (compare Jaillais *et al.* 2008) and our data indicate that the staining results vary between lots (see material and methods).

The electron micrographs suggest that organelles (vesicles) involved in wound healing fuse heterotypically with each other not only at or within the wound wall but already on their way towards the injured area. This would explain why FM1-43-derived fluorescence is observed on secretory vesicles in the wound cytoplasm in contrast to undisturbed cells where FM-dyes do not stain secretory vesicles visualized by DIC as long as the incubation time does not exceed two hours (Klima & Foissner 2008). We can, however, not exclude that the observed “fusion stages” represent budding vesicles.

Actin-dependent motility and deposition of organelles at wounds

The accumulation and deposition of FM1-43-stained and other organelles at wounds was inhibited by CD, which affects the actin cytoarchitecture, and by BDM, which interferes with actin-myosin interaction. This and the trajectories of organelles in the wound cytoplasm suggest that transport of putative endosomes and ER in the injured area occurs along the newly formed actin meshwork via myosin interaction as described for secretory vesicles (Foissner *et al.* 1996). It must be stated, however, that BDM is not considered to be an effective and specific inhibitor of *Chara* myosin (compare McCurdy 1999, Funaki et al. 2004). The cytoplasm at healing wounds is devoid of microtubules (Foissner & Wasteneys 1994) ruling out the possibility that the microtubular cytoskeleton is involved in organelle motility. Similar rearrangements of the actin and the microtubule cytoskeleton have been observed at sites of pathogen entry (Schmidt & Panstruga 2007) and even in cells which were only locally stimulated by touching the surface with fine glass or tungsten needles (Hardham *et al.* 2008). In an earlier study, the material present between the wound plug and the inner wound wall of punctured cells was interpreted as remnants of cytoplasm damaged during and after injury (Foissner 1988b). Here we prove that this material is actively deposited.

Constitutive internalization of FM-dyes in unwounded internodal cells is active but independent of an intact actin cytoskeleton, of actin-myosin interaction and of actin comets (Klima & Foissner 2008). This does not exclude that endocytosis at wounds is actin-dependent. CD primarily affects the deposition of the outer wound wall, a prerequisite for plasma membrane repair and it remains unclear whether or how actin filaments contribute to the formation and detachment of numerous coated vesicles in later stages of wound healing. These coated vesicles could be responsible for the diffuse FM1-43-fluorescence at healing wounds (compare Meckel et al. 2004).

The role of the endoplasmic reticulum

The deposition of huge membrane-bound compartments has been described from electron micrographs of wounds induced by Ca^{2+}-ionophores (Foissner 1988a; 1991). These cisternae were presumed to be of ER origin and cytochemical analysis indicated that they

were heavily loaded with Ca^{2+} (Foissner 1998). During this study we used CLSM of $DiOC_6$-labelled cells and prove that these cisternae are indeed of ER origin and that they are actively transported towards wounds and deposited. Wounding causes in influx of external calcium ions into the cell and it had been speculated that the accumulation of excess cytosolic Ca^{2+} by ER cisternae and their subsequent deposition helps to restore and maintain Ca^{2+} homoeostasis (Foissner 1991). The results of this study add support to this hypothesis and indicate that the deposition of ER cisternae into the extracytoplasmic space can be considered as an emergency mechanism required during early staging of wound healing and that the thickness of the outer wound wall reflects the level of Ca^{2+}-stress. Consistent with these observations, plasma membrane repair and the beginning of the deposition of the inner wound wall, during which exocytosis is coupled to endocytosis via coated vesicles, coincides with the recovery of membrane potential and membrane conduction (Homblé & Foissner 1993). Callose, the characteristic polysaccharide of the outer wound wall and known to be produced under high cytosolic Ca^{2+} (Colombani *et al.* 2004) is then replaced by cellulose in the inner wound wall. Intense ER accumulation, but no deposition, occurs in mechanically disturbed cells (Hardham *et al.* 2008) and in epidermal cells around lesions caused by pathogen attacks (Takemoto *et al.* 2006).

Supplementary Material

Refer to Web version on PubMed Central for supplementary material.

Acknowledgments

We thank Patric Schmölzer and Christian Pritz for stimulating discussions.

Abbreviations

BDM	2,3-butanedione monoxime
CD	cytochalasin D
CLSM	confocal laser scanning microscope/microscopy
DIC	differential interference contrast
$DiOC_6$	3,3′-dihexyloxacarbocyanine iodide
DMSO	dimethyl sulfoxide
ER	endoplasmic reticulum
LTred	LysoTracker Red

REFERENCES

Ayscough KR. Coupling actin dynamics to the endocytic process in *Saccharomyces cerevisiae*. Protoplasma. 2005; 226:81–88. [PubMed: 16231104]

Baluska F, Hlavacka A, Samaj J, Palme K, Robinson DG, Matoh T, McCurdy DW, Menzel D, Volkmann D. F-actin-dependent endocytosis of cell wall pectins in meristematic root cells. Insights from brefeldin A-induced compartments. Plant Physiology. 2002; 130:422–431. [PubMed: 12226521]

Colombani A, Djerbi S, Bessueille L, Blomqvist K, Ohlsson A, Berglund T, Teeri TT, Bulone V. In vitro synthesis of (1 -> 3)-beta-D-glucan (callose) and cellulose by detergent extracts of membranes from cell suspension cultures of hybrid aspen. Cellulose. 2004; 11:313–327.

Dettmer J, Hong-Hermesdorf A, Stierhof YD, Schumacher K. Vacuolar H^+-ATPase activity is required for endocytic and secretory trafficking in *Arabidopsis*. Plant Cell. 2006; 18:715–730. [PubMed: 16461582]

Dhonukshe P, Baluska F, Schlicht M, Hlavacka A, Samaj J, Friml J, Gadella TWJ. Endocytosis of cell surface material mediates cell plate formation during plant cytokinesis. Developmental Cell. 2006; 10:137–150. [PubMed: 16399085]

Dhonukshe P, Aniento F, Hwang I, Robinson D, Mravec J, Stierhof Y, Friml J. Clathrin-mediated constitutive endocytosis of PIN auxin efflux carriers in *Arabidopsis*. Current Biology. 2007; 17:520–527. [PubMed: 17306539]

Engqvist-Goldstein AEY, Drubin DG. Actin assembly and endocytosis: From yeast to mammals. Annual Review of Cell and Developmental Biology. 2003; 19:287–332.

Foissner I. Chlortetracycline-induced formation of wall appositions (callose plugs) in internodal cells of *Nitella flexilis* (Characeae). Journal of Phycology. 1988a; 24:458–467.

Foissner I. The relationship of echinate inclusions and coated vesicles on wound healing in *Nitella flexilis* (Characeae). Protoplasma. 1988b; 142:164–175.

Foissner I. Wall appositions induced by ionophore A 23187, $CaCl_2$, $LaCl_3$, and nifedipine in characean cells. Protoplasma. 1990; 154:80–90.

Foissner I. Induction of exocytosis in characean internodal cells by locally restricted application of chlortetracycline and the effect of cytochalasin B, depolarizing and hyperpolarizing agents. Plant, Cell and Environment. 1991; 14:907–915.

Foissner I. Localization of calcium ions in wounded characean internodal cells. New Phytologist. 1998; 139:449–458.

Foissner I. Microfilaments and microtubules control the shape, motility, and subcellular distribution of cortical mitochondria in characean internodal cells. Protoplasma. 2004; 224:145–157. [PubMed: 15614475]

Foissner I, Lichtscheidl IK, Wasteneys GO. Actin-based vesicle dynamics and exocytosis during wound wall formation in characean internodal cells. Cell Motility and the Cytoskeleton. 1996; 35:35–48. [PubMed: 8874964]

Foissner I, Menzel D, Wasteneys GO. Microtubule-dependent motility and orientation of the cortical endoplasmic reticulum in elongating characean internodal cells. Cell Motility and the Cytoskeleton. 2009; 66:142–155. [PubMed: 19137584]

Foissner I, Wasteneys GO. Injury to *Nitella* internodal cells alters microtubule organization but microtubules are not involved in the wound response. Protoplasma. 1994; 182:102–114.

Foissner I, Wasteneys GO. A cytochalasin-sensitive actin filament meshwork is a prerequisite for local wound wall deposition in *Nitella* internodal cells. Protoplasma. 1997; 200:17–30.

Foissner, I.; Wasteneys, GO. Actin in characean internodal cells. In: Staiger, C.; Baluska, F.; Volkmann, D.; Barlow, PW., editors. Actin: A dynamic framework for multiple plant cell functions. Kluwer Academic Publishers; Dordrecht, Boston, London: 2000. p. 259-274.

Foissner I, Wasteneys GO. Wide-ranging effects of eight cytochalasins and latrunculin A and B on intracellular motility and actin filament reorganization in characean internodal cells. Plant and Cell Physiology. 2007; 48:585–597. [PubMed: 17327257]

Franceschi VR, Lucas WJ. The glycosome of *Chara*: Ultrastructure, development, and composition. Journal of Ultrastructure Research. 1981; 75:218–228. [PubMed: 6167739]

Funaki K, Nagata A, Akimoto Y, Shimada K, Ito K, Yamamoto K. The motility of *Chara corallina* myosin was inhibited reversibly by 2,3-butanedione monoxime (BDM). Plant and Cell Physiology. 2004; 45:1342–1345. [PubMed: 15509860]

Galletta BJ, Cooper JA. Actin and endocytosis: mechanisms and phylogeny. Current Opinion in Cell Biology. 2009; 21:20–27. [PubMed: 19186047]

Graham LE, Cook ME, Busse JS. The origin of plants: Body plan changes contributing to a major evolutionary radiation. Proceedings of the National Academy of Sciences USA. 2000; 97:4535–4540.

Geldner N, Jürgens G. Endocytosis in signalling and development. Current Opinion in Plant Biology. 2006; 9:589–594. [PubMed: 17011816]

Griffing LR. FRET analysis of transmembrane flipping of FM4-64 in plant cells: is FM4-64 a robust marker for endocytosis? Journal of Microscopy. 2008; 231:291–298. [PubMed: 18778427]

Hardham A, Takemoto D, White R. Rapid and dynamic subcellular reorganization following mechanical stimulation of *Arabidopsis* epidermal cells mimics responses to fungal and oomycete attack. BMC Plant Biology. 2008; 8:63. [PubMed: 18513448]

Herth W, Schnepf E. The fluorochrome, calcofluor white, binds oriented to structural polysaccharide fibrils. Protoplasma. 1980; 105:129–133.

Homblé F, Foissner I. Electron microscopy and electrophysiology of local cell wall formation in *Chara corallina*. Plant Cell Physiology. 1993; 34:1283–1289.

Jaillais Y, Fobis-Loisy I, Miege C, Gaude T. Evidence for a sorting endosome in *Arabidopsis* root cells. Plant Journal. 2008; 53:237–247. [PubMed: 17999644]

Jelinkova A, Malinska K, Simon S, Kleine-Vehn J, Parezova M, Pejchar P, Kubes M, Martinec J, Friml J, Zazimalova E, Petrasek J. Probing plant membranes with FM dyes: tracking, dragging or blocking? Plant Journal. 2010; 61:883–892. [PubMed: 20003134]

Klima A, Foissner I. FM dyes label sterol-rich plasma membrane domains and are internalized independently of the cytoskeleton in characean internodal cells. Plant Cell Physiology. 2008; 49:1508–1521. [PubMed: 18757863]

McCurdy DW. Is 2,3-butanedione monoxime an effective inhibitor of myosin-based activities in plant cells? Protoplasma. 1999; 209:120–125. [PubMed: 18987800]

Meckel T, Hurst AC, Thiel G, Homann U. Endocytosis against high turgor: intact guard cells of *Vicia faba* constitutively endocytose fluorescently labelled plasma membrane and GFP-tagged K^+-channel KAT1. Plant Journal. 2004; 39:182–193. [PubMed: 15225284]

Meyer D, Pajonk S, Micali C, O'Connell R, Schulze-Lefert P. Extracellular transport and integration of plant secretory proteins into pathogen-induced cell wall compartments. Plant Journal. 2009; 57:986–999. [PubMed: 19000165]

Ovecka M, Lang I, Baluska F, Ismail A, Illes P, Lichtscheidl IK. Endocytosis and vesicle trafficking during tip growth of root hairs. Protoplasma. 2005; 226:39–54. [PubMed: 16231100]

Pickett JA, Edwardson JM. Compound exocytosis: Mechanisms and functional significance. Traffic. 2006; 7:109–116. [PubMed: 16420520]

Plattner, H.; Zingsheim, H-P. Elektronenmikroskopische Methodik in der Zell- und Molekularbiologie. Fischer; Stuttgart: 1987.

Reichardt I, Stierhof Y-D, Mayer U, Richter S, Schwarz H, Schumacher K, Jürgens G. Plant cytokinesis requires de novo secretory trafficking but not endocytosis. Current Biology. 2007; 17:2047–2053. [PubMed: 17997308]

Sachs, L. Angewandte Statistik. Springer; Berlin, Heidelberg, New York, Tokyo: 1984.

Samaj J, Müller J, Beck M, Bohm N, Menzel D. Vesicular trafficking, cytoskeleton and signalling in root hairs and pollen tubes. Trends in Plant Science. 2006; 11:594–600. [PubMed: 17092761]

Schapire AL, Valpuesta V, Botella MA. Plasma membrane repair in plants. Trends in Plant Science. 2009; 14:645–652. [PubMed: 19819752]

Schmidt SM, Panstruga R. Cytoskeleton functions in plant-microbe interactions. Physiological and Molecular Plant Pathology. 2007; 71:135–148.

Shimmen T, Yokota E. Cytoplasmic streaming in plants. Current Opinion in Cell Biology. 2004; 16:68–72. [PubMed: 15037307]

Stone BA, Evans NA, Bonig I, Clarke AE. The application of sirofluor, a chemically defined fluorochrome from aniline blue for the histochemical detection of callose. Protoplasma. 1984; 122:191–195.

Sun YD, Martin AC, Drubin DG. Endocytic internalization in budding yeast requires coordinated actin nucleation and myosin motor activity. Developmental Cell. 2006; 11:33–46. [PubMed: 16824951]

Takemoto D, Jones DA, Hardham AR. Re-organization of the cytoskeleton and endoplasmic reticulum in the Arabidopsis pen1-1 mutant inoculated with the non-adapted powdery mildew pathogen, *Blumeria graminis* f. sp hordei. Molecular Plant Pathology. 2006; 7:553–563. [PubMed: 20507469]

Turmel M, Pombert JF, Charlebois P, Otis C, Lemieux C. The green algal ancestry of land plants as revealed by the chloroplast genome. International Journal of Plant Sciences. 2007; 168:679–689.

van Gisbergen PAC, Esseling-Ozdoba A, Vos JW. Microinjecting FM4-64 validates it as a marker of the endocytic pathway in plants. Journal of Microscopy-Oxford. 2008; 231:284–290.

Voigt B, Timmers ACJ, Samaj J, Hlavacka A, Ueda T, Preuss M, Nielsen E, Mathur J, Emans N, Stenmark H, Nakano A, Baluska F, Menzel D. Actin-based motility of endosomes is linked to the polar tip growth of root hairs. European Journal of Cell Biology. 2005; 84:609–621. [PubMed: 16032929]

Europe PMC Funders Author Manuscripts

Europe PMC Funders Author Manuscripts

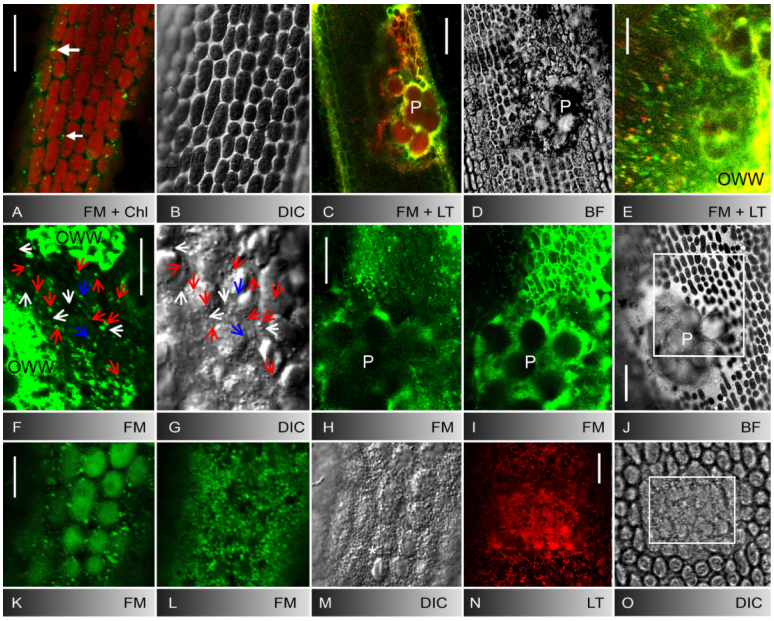

Fig. 1.

Control internodal cell of *Nitella flexilis* (A, B) and deposition of putative endosomes, acidic organelles and secretory vesicles at puncture (C-J) and UV-induced wounds (K-O). **A, B** FM1-43-staining pattern in the cortex 5 min after pulse-labelling (A) and corresponding bright field image (B). Few stable patches (large arrow) are visible at the plasma membrane and mobile organelles (small arrow) are seen between the autofluorescent chloroplasts. **C-E** Puncture wound of a cell stained with FM1-43 and LTred. LTred labels the solid inclusions of the wound plug (P in C and the bright field image D) and partly colocalizes with FM1-43-fluorescent organelles which accumulate at the wound (E) and are deposited as an outer wound wall (OWW). **F, G** FM1-43-stained organelles (F) and secretory vesicles visualized by DIC (G) in the wound cytoplasm beneath the brightly fluorescent outer wound wall (OWW). Blue arrows mark organelles visible only by FM1-43 fluorescence, white arrows mark organelles visible only by DIC, red arrows indicate colocalizations. **H-J** FM1-43-stained deposits (outer wound wall) beneath the wound plug (P) 5 min (H) and 20 min after puncturing (I). Rectangle in the bright field image J indicates area shown in H and I at higher magnification. **K-M** Cortical cytoplasm before (K) and after 5 min UV irradiation (L, M). FM1-43-stained organelles (L) and secretory vesicles (M) migrated towards the cell periphery where they form the outer wound wall. **N, O** UV-induced deposit of LTred-stained material (N) and of secretory vesicles (O) after 4 min irradiation in the boxed area. OWW = outer wound wall. Bars are 10 μm (E-G, K-O) and 25 μm (A-D, H-J)

Europe PMC Funders Author Manuscripts

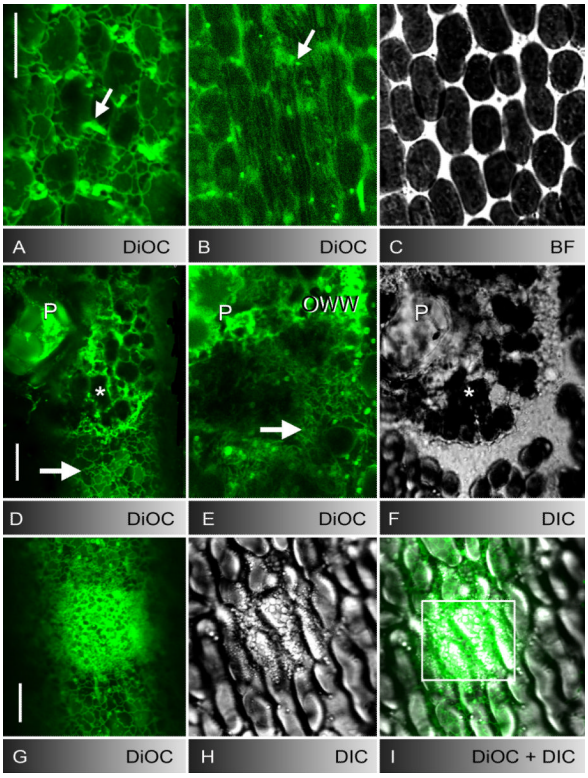

Fig. 2.

ER in control cells (A-C), at puncture (D-F) and UV-induced wounds (G-I). **A-C** $DiOC_6$-stained cortical ER meshwork (A), subcortical ER tubes (B), and mitochondria (arrows) in unwounded cell regions and corresponding bright field image of cortical chloroplasts (C). **D-F** $DiOC_6$-fluorescence (D and deeper optical section E) and DIC image (F) of a puncture wound. The wound plug (P) and cortical chloroplasts (asterisks) are surrounded and covered by brightly stained ER-remnants. The cortical ER in the unwounded control region (arrow in D) and the inner ER beneath the wound surface (arrow in E) is reticulate (compare with the tubular ER in control region B). **G-I** Accumulation of $DiOC_6$-stained ER (G) and secretory vesicles (H) after 4 min UV-irradiation in the boxed area of the merged image I. Bars are 10 μm

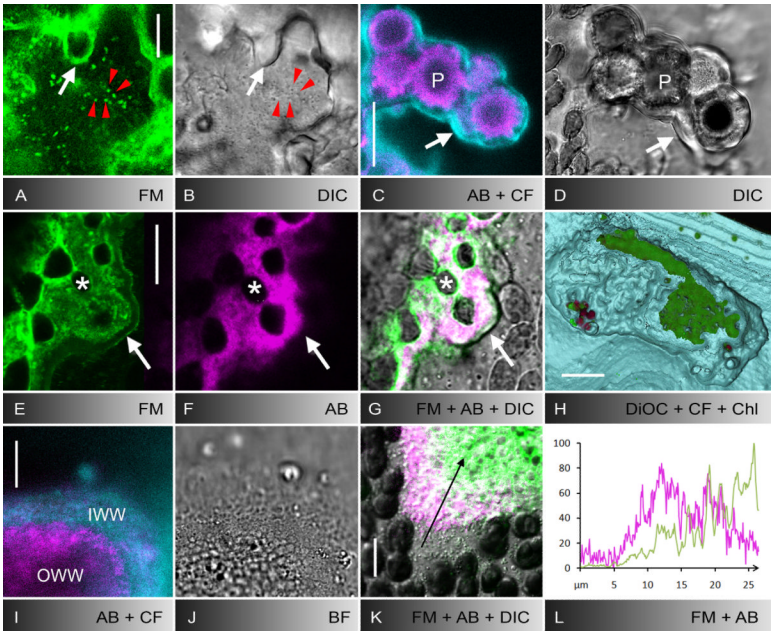

Fig. 3.

Secretion of the inner wound wall and polysaccharide components of wound walls induced by puncturing (A-H) or UV-irradiation (I-L). **A, B** FM1-43-stained organelles (A) and secretory vesicles visualized by DIC (B) during secretion of the inner wound wall about 30 minutes after puncturing. White arrows indicate FM1-43-fluorescent outer wound wall, red arrow heads indicate secretory vesicles which are labelled by FM-143. **C-G** Polysaccharide components of puncture wound walls. The outer wound wall adjacent to the wound plug (P) and to damaged chloroplasts (asterisks) is stained by aniline blue, indicative of callose (magenta in C, F, G). The inner wound wall is labelled by calcofluor, indicative of cellulose (cyan in C). White arrows indicate the border of the inner wound wall in the fluorescence images C, E and F and in the corresponding DIC (D) or bright field images (G, merged with E and F). Note FM1-43-stained plasma membrane along the inner wound wall (E) and colocalization of FM1-43-stained material and callose in the outer wound wall (E-G). **H** 3-D model of a puncture wound showing $DiOC_6$-stained ER deposits in the outer wound wall (green) covered by the calcofluor-labelled inner wound wall which is continuous with the normal cell wall (cyan). The wound is shown from the inside of the cell with peripheral layers cut off. Some autofluorescent chloroplasts adhere to the inner wound surface (red). **I-L** Polysaccharide components of UV-induced wound walls and colocalization with FM1-43-stained material. The outer wound wall contains callose (magenta in I) and the inner wound wall contains cellulose (cyan in I; J is the corresponding bright field image). Note that in this glancing optical section the inner wound wall appears thicker than it is. Callose (magenta) partly colocalizes with the FM1-43-fluorescent material (green) in the outer wound wall (K, merged with DIC). The graph in L shows the normalized intensity distributions of FM1-43 (green) and aniline blue fluorescence (magenta) along the arrow in K. Bars are 10 µm (A, B, I-K), 25 µm (C-G) and 100 µm (H)

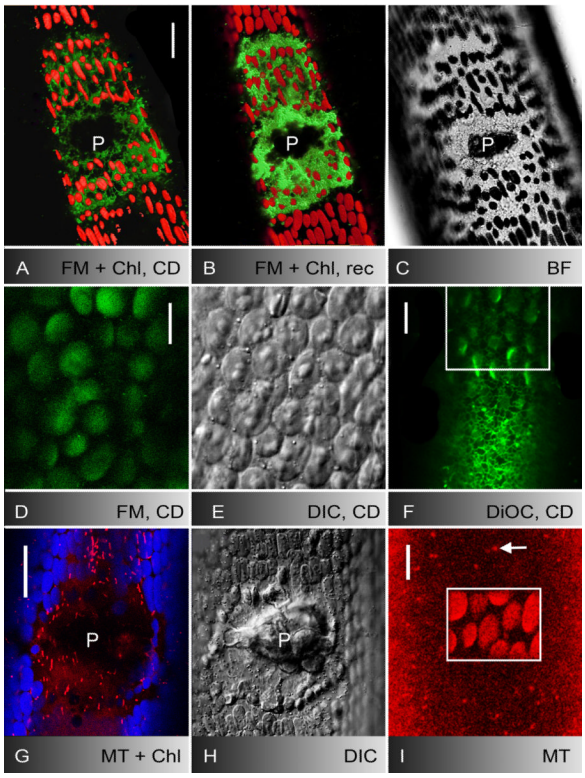

Fig. 4.

Actin-dependent deposition of FM1-43-stained membranes, secretory vesicles and ER cisternae at puncture (A-C) and UV-induced wounds (D-F) and behaviour of mitochondria (G-I). **A-C** FM1-43-stained membranes and autofluorescent chloroplasts in the outer wound wall one hour after puncturing in cytochalasin D (CD; A) and after two hours recovery in AFW (B; D is the corresponding bright field image). Note increase in FM1-43-fluorescence (A and B are 3-D projections of about 40 optical sections). **D-F** CD inhibits the migration and deposition of FM1-43-stained organelles (D), of secretory vesicles (E) and of $DiOC_6$-stained ER cisternae (F) towards UV-induced wounds (images were taken after 5 min irradiation). Cortical ER is seen outside the irradiated area (boxed) in F. **G-I** Mitochondria labelled by mitotracker orange (red) are neither deposited at puncture wounds (autofluorescent chloroplasts are shown in blue; H is the corresponding DIC image) nor at UV-induced wounds (boxed area in I; damaged chloroplasts show enhanced autofluorescence). The arrow points to a cortical mitochondrion outside the irradiated area. P = wound plug. Bars are 10 (D-F and I) and 25 μm (A-C, G and H)

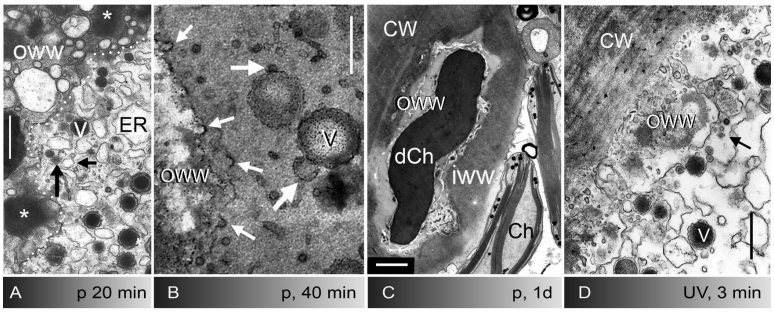

Fig. 5.

Fine structure of puncture- (A-C) and UV-induced wounds (D) in internodal cells of *Nitella flexilis*. **A-C** Puncture wound healing. **A** Deposition of the outer wound wall (OWW). The border between the outer wound wall and the wound cytoplasm which contains ER cisternae, secretory vesicles (V) and other vesicles (arrows) is indicated by a puncture line. The asterisk marks the content of secretory vesicles in the outer wound wall. **B** Numerous coated pits (small arrows) are visible at the newly formed plasma membrane during secretion of the inner wound wall. Large arrows indicate putative fusion stages between different kinds of vesicles. Electron dense deposits are indicative of polysaccharides. **C** Healed puncture wound. A bipartite wound wall covers a damaged chloroplast (dCh), an intact chloroplast (Ch) is seen in the cytoplasm. CW = normal cell wall, IWW = inner wound wall, OWW = outer wound wall. **D** UV-induced wound. Numerous coated vesicles (arrow) pinch off the plasma membrane prior to and during the deposition of the inner wound wall. Cells were fixed 20 min (A), 40 min (B) and one day after puncturing (C) and after 5 min recovery from 4 min irradiation with UV (D). Bars are 500 nm (A-B, D) and 1 μm (C)

Europe PMC Funders Author Manuscripts

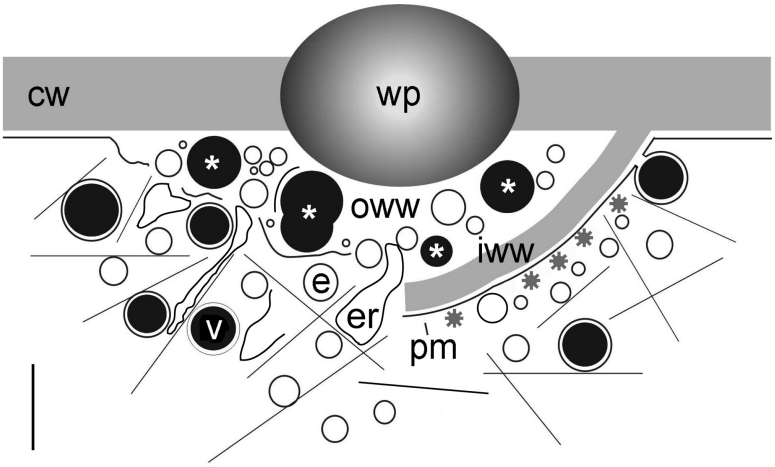

Fig. 6.

Schematic representation of puncture wound healing. Left: Deposition of the outer wound wall (OWW). Secretory vesicles (V), putative recycling endosomes (E) and cisternae of the endoplasmic reticulum (ER) move along actin filaments (thin lines) and fuse with each other at the inner surface of the wound plug (P). Their membranes are not recycled and remain either trapped between clumps of amorphous polysaccharides (content of secretory vesicles; asterisks) or provide the material required for plasma membrane repair. Right: Secretion of the cellulosic inner wound wall (IWW). Exocytosis of secretory and other vesicles with the newly formed plasma membrane (PM) is coupled with endocytosis via coated vesicles. CW = cell wall. Bar is approximately 1 μm

Europe PMC Funders Author Manuscripts

Table 1

Volume of FM1-43-fluorescent material at wounds punctured (p) in the presence of cytochalasin D (CD) and after recovery from CD treatment in artificial fresh water (AFW). Values are based on z-stacks taken with identical settings for reference (CD, p, CD 1h) and treatments (recovery in AFW or, respectively, prolonged treatment with CD). The decreased volume in cells treated with CD for 4 h after puncturing is due to bleaching of the FM1-43-fluorescence. Data are normalized and given as means of triplicates±SD.

	CD, p, CD 1h	CD, p, CD1h, AFW 3h	CD, p, CD 4h
Chara corallina	100±0	192,4±55,9	28,3±28,3
Nitella flexilis	100±0	141,1±18,3	34,1±13,0